

Biocompatible gold nanorods: One-step surface functionalization, highly colloidal stability, and low cytotoxicity

Author:

Liu, K; Zheng, Y; Lu, X; Thai, T; Lee, NA; Bach, U; Gooding, JJ

Publication details:

Langmuir

v. 31

Chapter No. 17

Medium: Print-Electronic

pp. 4973 - 4980

0743-7463 (ISSN); 1520-5827 (ISSN)

Publication Date:

2015-05-05

Publisher DOI:

<https://doi.org/10.1021/acs.langmuir.5b00666>

License:

<https://creativecommons.org/licenses/by-nc-nd/4.0/>

Link to license to see what you are allowed to do with this resource.

Downloaded from http://hdl.handle.net/1959.4/unsworks_55312 in <https://unsworks.unsw.edu.au> on 2024-05-03

Biocompatible Gold Nanorods: One-step Surface Functionalization, Highly Colloidal Stability and Low Cytotoxicity

Kang Liu,^{†,§} Yuanhui Zheng,^{†,} Xun Lu,[†] Thibaut Thai,[‡] Nanju Alice Lee,[§] Udo Bach[‡] and J. Justin Gooding^{†,#,*}*

[†]School of Chemistry and Australian Centre for NanoMedicine, The University of New South Wales, Sydney, NSW 2052, Australia

[‡]Department of Materials Engineering, Monash University, Wellington Road, Clayton, Victoria 3800, Australia

[§]ARC Training Centre for Advanced Technologies in Food Manufacture (ATFM), School of Chemical Engineering, The University of New South Wales, Sydney, NSW 2052, Australia

[#]ARC Centre of Excellence in Convergent Bio-Nano Science and Technology, School of Chemistry, The University of New South Wales, Sydney, NSW 2052, Australia

Keywords: gold nanorods, surface modification, PEGylation, silver etching, detoxification

ABSTRACT: The conjugation of gold nanorods (AuNRs) with polyethylene glycol (PEG) is one of the most effective ways to reduce their cytotoxicity arising from the cetyltrimethylammonium bromide (CTAB) and silver ions used in their synthesis. However, typical PEGylation occurs only

at the tips of the AuNRs, producing partially modified AuNRs. To address this issue, we have developed a novel, facile, one-step surface functionalization method that involves the use of Tween 20 to stabilize AuNRs, bis(p-sulfonatophenyl)phenylphosphine (BSPP) to activate the AuNR surface for the subsequent PEGylation, and NaCl to etch silver from the AuNRs. This method allows for the complete removal of the surface-bound CTAB and the most active surface silver from the AuNRs. The produced AuNRs showed far lower toxicity than other methods to PEGylate AuNRs, with no apparent toxicity when their concentration is lower than 5 $\mu\text{g/mL}$. Even at a high concentration of 80 $\mu\text{g/mL}$, their cell viability is still four times higher than that of the tip-modified AuNRs.

1. INTRODUCTION

Gold nanorods (AuNRs) have received a tremendous amount of interest of late in the fields of plasmonics,¹⁻³ molecular sensing,⁴⁻⁶ and hyperthermia-based cancer therapy.⁷⁻¹⁰ Their anisotropic geometry provides them with an exceptional spectral response in the visible and near infrared range, which originates from the excitation of transverse and longitudinal modes of the localized surface plasmons along the short and long axes, respectively.⁸ The most common method to produce a high yield of AuNRs is the seed-mediated synthesis that involves the use of cetyltrimethylammonium bromide (CTAB) and silver nitrate to control over nanorod formation and aspect ratio.¹¹⁻¹³ The CTAB tightly adsorbs on the gold surface to form a dense surface-confined cationic bilayer with the trimethylammonium head facing the external environment. This makes it difficult to remove CTAB without causing nanorod aggregation. On the other hand, it has been shown that, during the AuNR synthesis, silver ions are reduced and deposited on the gold surface in the form of atomic silver monolayers or sub-monolayers at a potential much less negative than bulk reduction, known as underpotential deposition.¹⁴ Recently, Jackson *et al.*

experimentally observed that the silver atoms were located in the outermost ~2 nm surface layer of the AuNRs, rather than in the core.¹⁵ Under aerobic conditions, the surface silver atoms dissolve in aqueous solutions as a form of silver ions.¹⁶ This reaction is hindered to a large extent when AuNRs are coated with long chain organic molecules.¹⁷

Both CTAB and silver ions in the colloidal AuNR solution pose a threat to many biological systems, as they are known to be cytotoxic.^{9,14,18-23} It has been reported that CTAB can disrupt the lipid bilayer of cell membrane forming nanoscale holes within the membrane due to the electrostatic adsorption of quaternary ammonium cations onto the membrane, thus increasing its permeability.¹⁸ There is also an evidence that silver ions interact with cell membranes and lead to actin depolymerization in the cytoskeleton connecting tightly with the membrane, ultimately causing the cell death.²³ Therefore, the ability to completely remove CTAB, prevent silver ion leaching and maintain AuNR colloidal stability will be key requirements towards their in vivo diagnostic and therapeutic applications.

So far, considerable effort has been devoted to the development of surface functionalization strategies aiming at replacing CTAB with more biocompatible surface ligands, such as thiol-terminated polyethylene glycol (HS-PEG),^{20,24-27} alkanethiols,²⁸⁻³² thiolated CTAB analogues,³³ thiolated glycans³⁴ and phospholipids.^{35,36} Among these ligands, thiolated PEGs are the most widely used molecules as they provide AuNRs with a high degree of anti-fouling ability, colloidal stability and biocompatibility in biological media.^{20,24-27,29} Liao *et al.* developed a standard procedure for AuNR PEGylation via a one-step ligand exchange reaction (referred to as the Liao method).²⁷ This reaction can be significantly accelerated in the presence of tris-buffer with pH of 3.²⁶ The main drawback of this one-step PEGylation method is that only the more weakly bound CTAB molecules at the tips are displaced with thiolated PEG, producing partially functionalized

AuNRs.³⁷ To achieve higher PEGylation efficiency, Kinnear *et al.* recently established a two-step ligand exchange method that takes advantage of ethanol to desorb the CTAB from the sides of the partially modified AuNRs followed by another PEGylation step (referred to as the Kinnear method).²⁵ The authors claimed that this method enables the complete functionalization of AuNRs with thiolated PEG. However, a small quantity of CTAB was still observed on the AuNRs.²⁵ This may still cause cytotoxicity at an elevated AuNR concentration required for high cellular uptake of AuNRs.^{9,19,33}

Despite the above-mentioned advances, there are still several challenges for the surface modification of AuNRs with thiolated PEG. Firstly, the existing methods usually suffer from a low PEGylation efficiency,²⁶⁻²⁷ which can limit the effectiveness of the PEG layer as surface coverage has been shown to be important for the effectiveness of PEG layers.³⁸ Moreover, they are also quite complicated²⁵ or experience serious loss of AuNRs due to the irreversible nanorod aggregation during the purification process.²⁷ Therefore, a major goal of the field is to design a simple, reliable, robust functionalization procedure to produce colloiddally stable and biocompatible (i.e. CTAB free) AuNRs.

2. EXPERIMENTAL SECTION

Chemicals and Materials. All chemicals and reagents were purchased from Sigma-Aldrich and used as received, unless otherwise stated. Milli-Q water (18.2 M Ω) was used for all experiments.

Synthesis of CTAB-capped AuNRs. AuNRs with an average aspect ratio of 3.2 were synthesized by the seed-mediated method described by the group of El-Sayed.¹¹ In a typical procedure, a seed solution was prepared by adding an ice-cold NaBH₄ solution (0.6 mL, 0.01 M) into a mixture of CTAB solution (5 mL, 0.20 M) and HAuCl₄ (5 mL, 0.5 mM). The mixture was then vigorously stirred for 2 min, followed by an incubation at 30 °C for 2 h. A growth solution

(~60 mL) was made by successively adding 1.5 mL of AgNO₃ (4 mM), 30 mL of 1 mM of HAuCl₄, and 0.42 mL of 78.8 mM ascorbic acid into a 30 mL of 0.2 M CTAB solution. The color of the growth solution changed from yellow brown to colorless immediately. Subsequently, the seed solution (72 μL) was added to the growth solution and incubated at 30 °C overnight. The AuNRs were then purified by three centrifugation cycles (14800 rpm, 30 min, Sigma 1-14 Microfuge) to remove excess CTAB and unreacted products. After the final step of purification, the AuNRs were redispersed in ultrapure water.

Preparation of PEGylated AuNRs. In a typical procedure, AuNR PEGylation was conducted by successive addition of 5 μL of 2 vol% Tween 20 aqueous solution, 5 μL of 0.1 M bis(p-sulfonatophenyl)phenylphosphine dihydrate dipotassium salt (BSPP), 12.6 μL of 1.6 mM thiol-terminal polyethylene glycol (HS-PEG, MW ≈ 2000 g/mol, [HS-PEG]/[AuNR] = 1.24 × 10⁵), 50 μL of 2 M NaCl and 30 μL of water into a 100 μL of concentrated AuNR solution with an optical density (OD) of 9. The mixture was placed in a ThermoMixer C (Eppendorf) and incubated at room temperature for 24 h (mixing frequency: 900 rpm). The PEGylated AuNRs were purified by centrifugation (14800 rpm, 30 min) and redispersed ultrapure water.

For comparison, AuNRs were also PEGylated by the methods developed by Liao *et al.* (Liao method)²⁷ and Kinnear *et al.* (Kinnear method).²⁵

Liao method: 12.6 μL of 1.6 mM HS-PEG and 90 μL of water were added into a 100 μL of concentrated AuNR solution (OD = 9), followed by an incubation for 24 h (mixing frequency: 900 rpm). The PEGylated AuNRs were purified by centrifugation (14800 rpm, 30 min) and redispersed ultrapure water.

Kinnear method: 12.6 μL of 1.6 mM HS-PEG and 90 μL of water were added into a 100 μL of concentrated AuNRs solution ($\text{OD} = 9$), followed by an incubation for 24 h (mixing frequency: 900 rpm). The PEGylated AuNRs were washed with water for 3 times by centrifugation (14800 rpm, 30 min) and redispersed in 1 mL of ethanol (90 vol% ethanol in water). After that, a 12.6 μL of ethanolic solution of HS-PEG (1.6 mM in 90 vol% ethanol in water) was added, followed by an incubation for 24 h (mixing frequency: 900 rpm). The PEGylated AuNRs were purified by centrifugation (14800 rpm, 30 min) and redispersed ultrapure water.

Fabrication of Positively Charged Silicon Substrate. In a typical procedure, silicon substrates (purchased from UniversityWafers) were cleaned with Piranha solution for 30 min, washed with water three times and then dried under a stream of argon. The substrates were subsequently exposed to a mixture of 4 μL of (3-aminopropyl)triethoxysilane (APTES), 190 μL of ethanol and 6 μL of water for 1 h, washed with ethanol three times and then dried under a stream of argon. After that, the substrates were baked at 110 $^{\circ}\text{C}$ for 10 min.

Electrostatic Immobilization of AuNRs onto APTES-Modified Silicon Substrates. The electrostatic assembly of PEGylated AuNRs onto APTES-modified silicon substrates was performed in a petri dish where droplets of water were placed to maintain a constant humidity during the AuNR immobilization. 20 μL of completely PEGylated AuNR ($\text{OD} = 9$) solution was placed onto a positively charged substrate (i.e. APTES modified substrate) and left to incubate for 4 h. The substrate was thereafter dipped in and out three times in water to remove non-specific adsorbed AuNRs and dried under a stream of argon.

Cell culture. Human cervical cancer cells line (HeLa cells) were cultured in Dulbecco's modified Eagle's medium (DMEM, Life Technologies, 11885-084) supplemented with 10 vol% fetal bovine serum, 50 U/mL penicillin, and 50 mg/mL streptomycin.

3-(4,5-dimethylthiazol-2-yl)-2,5-diphenyltetrazolium bromide (MTT) assay. Cell toxicity was measured using the standard MTT assay. Note that the PEGylated AuNRs were purified by three centrifugation cycles after the surface functionalization with PEG (The AuNR solutions were diluted by 10 times after each centrifugation cycle). The free CTAB concentrations of the resulted AuNR solutions are estimated to be $\sim 1 \mu\text{M}$ for all the samples. The cytotoxicity of the PEGylated AuNRs was analyzed by using a HeLa cells line. The cells were seeded in 96-well flat bottom plates at a concentration of 3000 cells per well and were incubated for 24 h at 37 °C (constant temperature and humidity, 5% CO₂). Then, the PEGylated AuNRs with concentrations ranging from 1.25 to 80 $\mu\text{g/mL}$ were added into the plate wells. All these AuNR solutions were diluted from a DMEM solution containing 80 $\mu\text{g/mL}$ of the PEGylated AuNRs and $\sim 0.2 \mu\text{M}$ of free CTAB. The cells were further incubated for 24 h at 37 °C. Cell viability was determined by the addition of MTT (30 μL , 5 mg/mL in sterile phosphate buffered saline). The plates were further incubated for 4 h at 37 °C, allowing viable cells to convert the pale yellow MTT to an insoluble purple formazan. Then the medium was carefully removed and a 100 μL of dimethyl sulfoxide (DMSO) was added to dissolve the insoluble formazan reduced from MTT by living cells. The absorbance of the colored medium was measured at 550 nm by using a scanning multiwell spectrophotometer (FLUOstar Omega, BMG LABTECH). The viability of HeLa cells was also recorded by the morphological criteria using optical microscope. After treatment with PEGylated AuNRs for 4 h, the cell morphology was observed by bright-field microscopy (Leica DM IL LED inverted phase contrast microscope). The magnification was set at 200 \times for all samples.

Characterization. UV-Vis absorption spectra were obtained with a Shimadzu UV-2401PC UV-VIS spectrophotometer at room temperature. The concentration of AuNRs solution was determined by UV-VIS spectroscopy based on the experimental extinction coefficients previously reported.¹² Raman spectra were collected on a RamanMicro 300 Raman Microscope (Perkinelmer). For all Raman measurements, the samples were exposed to a near infrared diode laser ($\lambda_{\text{ex}} = 785 \text{ nm}$, $P_{\text{ex}} = 80 \text{ mW}$) for 4 s, and the Raman signals were collected from 5 scans. During the measurements, the laser beam was positioned through an Olympus imaging microscope objective lens (100 \times). For the Raman sample preparation, AuNRs was drop-cast onto a gold-coated silicon substrate (thickness of gold film: 30 nm) and then dried in air. All Raman spectra were taken from the “coffee-ring” area (see Figure S1, Supporting Information). Elemental analyses were conducted using X-ray photoelectron spectroscopy (XPS). A Kratos Axis ULTRA XPS incorporating 165 mm hemispherical electron energy was used. The incident radiation was monochromatic Al X-rays (1486.6 eV) at 225 W (15 kV, 15 ma). Survey (wide) scans were taken at an analyzer pass energy of 160 eV and multiplex (narrow) higher resolution scans at 20 eV. Survey scans were carried out over 1200 eV binding energy with 1.0 eV steps and a dwell time of 100 ms. Binding energy were calibrated with C1s peak at 285.0 eV to compensate for surface charging effect. Component fitting of the high-resolution spectra was performed using Avantage software. Silicon substrates were use as supporting substrates for the XPS measurements. All XPS spectra were taken from the “coffee-ring” area, as presented in Figure S1. For the Raman and XPS measurements, the PEGylated AuNRs were purified by eight centrifugation cycles after the surface functionalization with PEG (Note: The AuNR solutions were diluted by ~ 20 times after each centrifugation cycle). The Ag/Au elemental ratios of the samples were determined by means of inductively coupled plasma mass spectrometry (ICP-MS) (Perkin Elmer, NexION 300D with

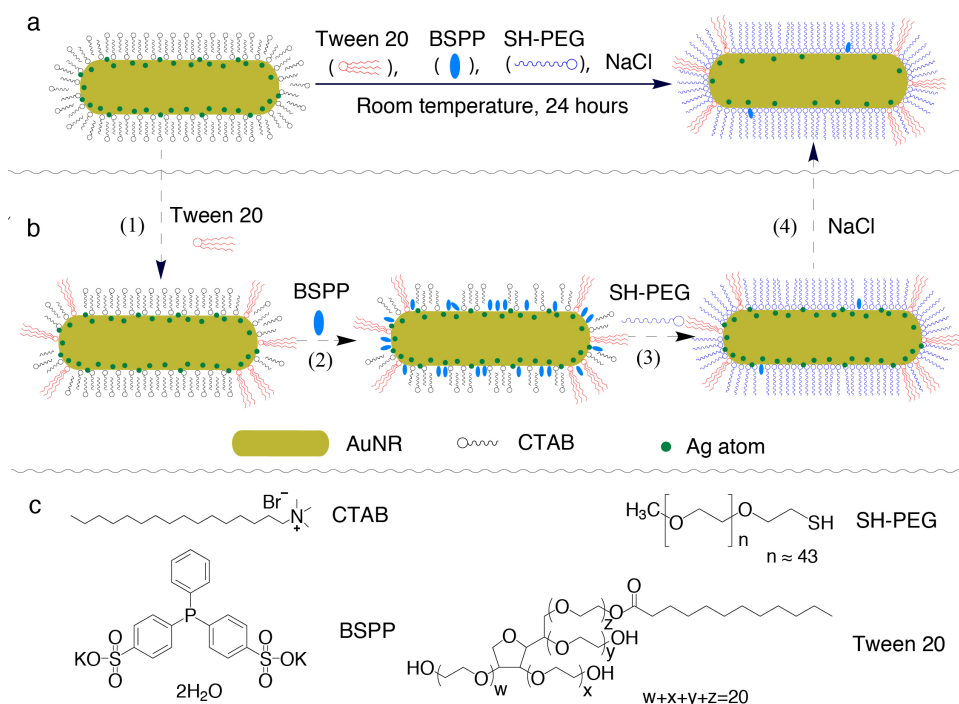
Universal cell technology). A 100 μL of concentrated AuNR solution ($\text{OD} = 9$) were diluted to 500 μL using 2 vol% HNO_3 . An aliquot of 200 μL of the diluted solution was further diluted to 500 μL with 2 vol% aqua regia, then analyzed by ICP-MS for Au content. Ag content was analyzed in a similar way except treating with 2 vol% HNO_3 . Scanning electron microscopy (SEM) images of the AuNRs were taken using a FEI NOVA 230 operating at 5 kV (Figure S2, Supporting Information).

3. RESULTS AND DISCUSSION

The purpose of this paper is to report a facile one-step AuNR PEGylation method that allows for the complete removal of surface-confined CTAB (Scheme 1). Experimentally, CTAB-capped AuNRs were synthesized through the seed-mediated method developed by the group of El-Sayed.¹¹ The as-synthesized AuNRs are 48.7 ± 4.1 nm in length and 15.3 ± 1.4 nm in width (Figure S2, Supporting Information). To effectively exchange the surface-confined CTAB with thiolated PEG, the concentration of free CTAB in the AuNR solution was lowered to a point (~ 1 mM) where the AuNRs are still colloidally stable and the surface ligand exchange is favorable. A further decrease of free CTAB concentration results in the irreversible aggregation of the AuNRs (Figure S3, Supporting Information).

Once the AuNRs were formed, the AuNR PEGylation was conducted with the successive addition of Tween 20, bis(p-sulfonatophenyl)phenylphosphine (BSPP), monothiol-PEG (HS-PEG, $M_w \approx 2000$ g/mol), and NaCl into the CTAB-capped AuNR solution, followed by an incubation at room temperature for 24 h (Scheme 1a). This method takes advantage of Tween 20 to stabilize AuNRs (step 1, scheme 1b), BSPP to activate the AuNR surface (step 2, scheme 1b) and NaCl to etch silver on the AuNR surface (step 4, scheme 1b). Tween 20, a nonionic and biocompatible surfactant, has been widely used as a stabilizer for the surface modification of gold nanoparticles

(AuNPs),³⁹ and halogens are known to etch silver NPs.⁴⁰ The reason for choosing BSPP as a surface activation agent is that (1) it is relatively small compared with the PEG molecule and can more easily penetrate through the CTAB bilayer to the AuNR surface, to which it readily chemisorbs; (2) it carries two charges that electrostatically stabilize AuNRs during the surface activation; and (3) the strength of gold-phosphine bond (13-20 kcal/mol)⁴¹ is in-between those of gold-nitrogen (8 kcal/mol)⁴² and gold-sulfur (40-50 kcal/mol) bonds, thus allowing it to displace the CTAB but itself be displaced by the HS-PEG.⁴³



Scheme 1. a) A schematic representation of the one-step surface functionalization of AuNRs with thiolated PEG: the PEGylation was conducted by successively adding surfactant Tween 20, bis(p-sulfonatophenyl)phenylphosphine dihydrate dipotassium (BSPP), HS-PEG and NaCl into a CTAB-capped AuNR solution, followed by an incubation at room temperature for 24 h, b) the proposed surface modification mechanism, and c) chemical structures of surface-active compounds. The components are not shown to scale

To gain further insight into the AuNR PEGylation mechanism, we modified AuNRs with HS-PEG following the procedure illustrated in Scheme 1a and compared them by leaving out some key components, such as Tween 20, BSPP and NaCl. The AuNRs PEGylated by our method show an increased colloidal stability against a concentrated saline buffer solution and multiple rounds of centrifugation compared with CTAB-capped ones. They are extremely stable in a solution containing 0.5 M NaCl and 20 mM phosphate buffer (pH, 7.5) while the CTAB-capped ones completely precipitated in the same medium within 1 h (Figure S3, Supporting Information). Without Tween 20, the PEGylated AuNRs tend to stick on the wall of centrifuge tubes during the purification process, resulting in a serious loss of AuNRs (Figure S3). Subjected to three centrifugation cycles, the loss of AuNR was 0.8% for our method, while it was 60% for the Liao method (no Tween 20).

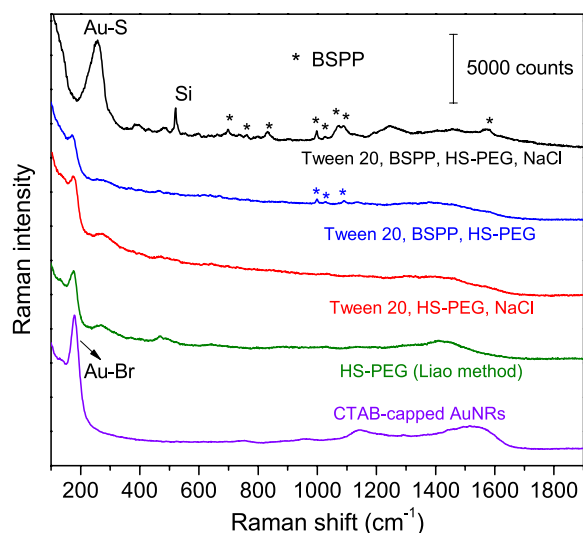


Figure 1. Raman spectra of PEGylated AuNRs prepared under conditions of Tween 20, BSPP, HS-PEG and NaCl (our method, black curve), Tween 20, BSPP and HS-PEG (blue curve), Tween 20, HS-PEG and NaCl (red curve) and HS-PEG (the Liao method, green curve). For comparison, the Raman spectrum of CTAB-capped AuNRs (violet curve) is provided as a reference.

Figure 1 shows the Raman spectra of the AuNRs before and after surface modification. All Raman spectra were taken from the “coffee-ring” area, where AuNRs are closely packed, to ensure sensitive and precise surface-plasmon enhanced Raman detection of the surface bound molecules (Figure S1, Supporting Information). As shown in Figure 1, there is only one Raman peak in the range of 100-400 cm^{-1} for the AuNRs prior to (i.e., CTAB-capped AuNRs, violet curve) and after the PEGylation by our method (black spectrum). The Raman peak at 182 cm^{-1} is assigned to the Au-Br bond, while the one at 250 cm^{-1} is ascribed to the Au-S bond.²⁶⁻²⁷ It has been suggested that CTAB adsorbed on the AuNR surface via a Au-Br-N bridge.⁴⁴ Upon the PEGylation, the Au-Br peak completely vanishes, suggesting that CTAB has been completely displaced by the PEG molecules. However, both of Au-Br and Au-S peaks are observed for the AuNRs PEGylated by the Liao method (green curve) and our method in the absence of NaCl (blue curve) or BSPP (red curve). It is worthwhile to mention that Liao *et al.* observed only Au-S peak rather than Au-Br and Au-S peaks in their Raman experiments.²⁷ This is because their spectrum was taken from isolated AuNRs²⁷ rather than from coupled AuNRs as we did here. For isolated AuNRs, the Raman hot spots locate at the tips of the AuNRs and only the molecules at the tips can be excited, while for coupled AuNRs (coffee ring area), as shown in Figure S1 in the Supporting Information, the Raman hot spots locate at the gaps between two adjacent AuNRs⁴⁵⁻⁴⁷ and the molecules at both tips and sides of the nanorods can be excited. For the AuNRs PEGylated by the Liao method, the observation of only Au-S peak from isolated nanorods and both Au-Br and Au-S peaks from the coupled ones further confirms that the Liao method produce only tip-modified AuNRs. A similar observation to the Liao method is made for the PEGylated AuNRs prepared using the Kinnear method (Figure S4, Supporting Information). In Kinnear’s work, the presence of CTAB and HS-PEG on the AuNR surface were revealed by nuclear magnetic resonance spectroscopy.²⁵ When

BSPP is used for the AuNR PEGylation, several new Raman peaks at e.g., 998, 1026 and 1089 cm^{-1} are observed (black and blue curves). These peaks stem from the vibration bands of phenyl ring of BSPP adsorbed on the AuNR surface,⁴⁸ suggesting that BSPP molecules penetrate through the CTAB bilayer and partially replace them (step 2, scheme 1b). The Raman signals of BSPP become stronger for the AuNRs PEGylated in the presence of NaCl (black curve) compared with in the absence of NaCl (blue curve), showing that NaCl facilitates the adsorption of BSPP onto the AuNRs and the removal of the CTAB.

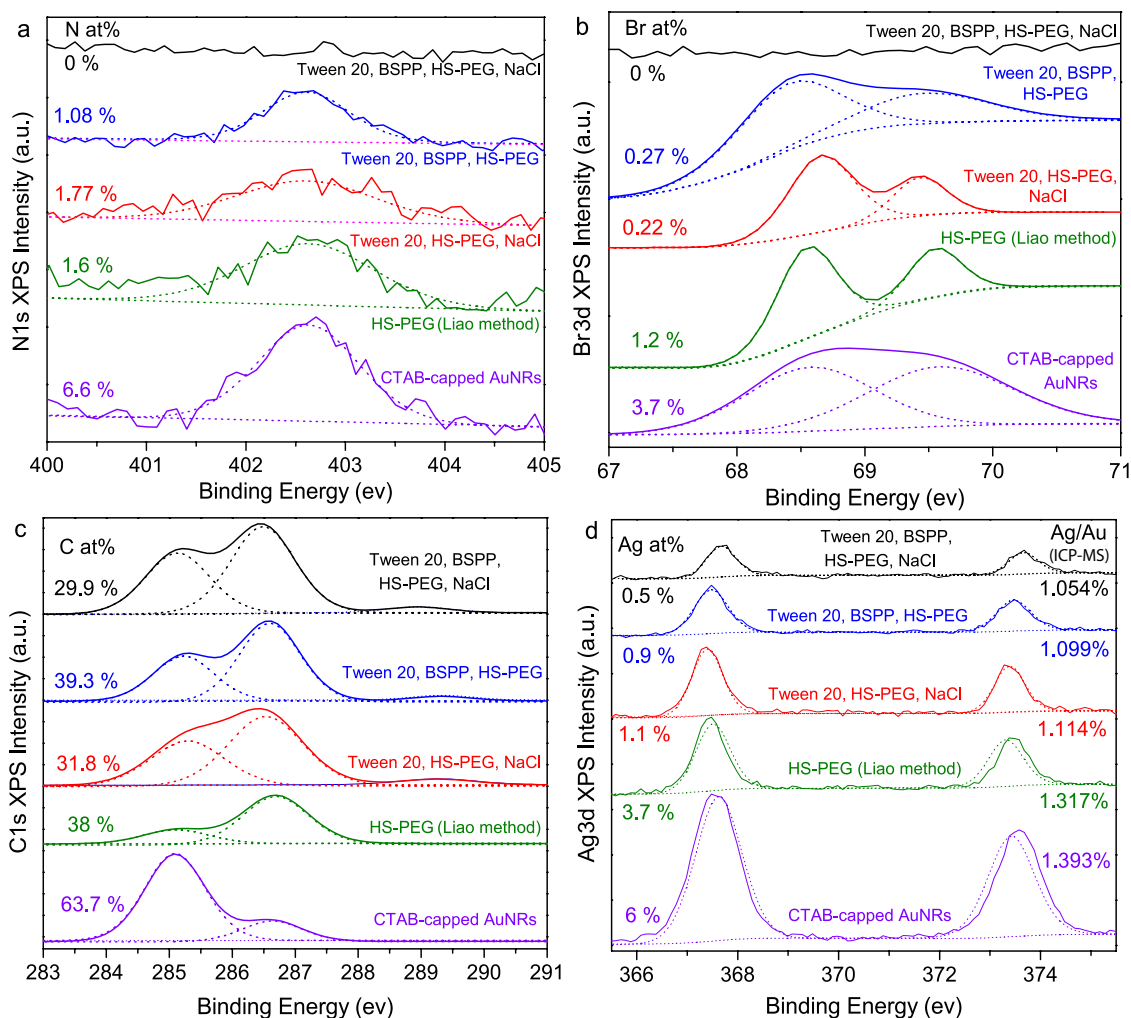


Figure 2. High-resolution a) N1s, b) Br3d, c) C1s, and d) Ag3d XPS spectra of PEGylated AuNRs synthesized under conditions of Tween 20, BSPP, HS-PEG and NaCl (our method; black curve),

Tween 20, BSPP and HS-PEG (blue curve), Tween 20, HS-PEG and NaCl (red curve), and HS-PEG (Liao method; green curve). For comparison, N1s, Br3d, C1s, and Ag3d spectra of CTAB-capped AuNRs (violet curves) are provided as references. The atomic percentage of N, Br, C and Ag obtained from XPS survey spectra (Figure S5, Supporting Information) are listed in the corresponding panels. The Ag/Au ratio obtained from ICP-MS measurements are also listed in panel d.

Figure 2 shows high-resolution N1s, Br3d, C1s and Ag3d XPS spectra of the PEGylated AuNRs. In Figure 2a and b, both N1s (402.6 eV) and Br3d (68.6 and 69.6 eV) peaks are absent for the AuNRs PEGylated by our method (black curve) but if no NaCl (blue curve) or BSPP (red curve) is used, or in the case of the Liao method (green curve) they are observed. This reveals that our method is capable of completely removing CTAB molecules from the AuNRs. The PEGylation efficiency (defined as $\eta = (C_0 - C)/C_0 \times 100\%$, where C_0 is the amount of CTAB bound to the original AuNRs and C is the amount of CTAB remaining on the AuNRs after PEGylation as determined using the nitrogen contents obtained from the XPS measurements derived from the CTAB) is calculated to be 52% (the Liao method), 46% (without BSPP), 67% (without NaCl) and 100% (our method) (see Supporting Information for calculation details). The higher PEGylation efficiency for AuNRs modified in the presence of BSPP further confirms that BSPP serves as a surface activation agent for the AuNR PEGylation, which is in good agreement with the Raman results shown in Figure 1.

High-resolution C1s spectra (Figure 2c) show two peaks at 285.0 and 286.5 eV that are assigned to C-C and C-O bonds for all samples. The C-O peak observed in the CTAB-capped AuNRs (violet curve) might arise from adventitious carbon contaminants while the C-C peak is derived mainly

from the alkyl chain of CTAB. A new C1s peak at 288.5 eV is observed from the AuNRs PEGylated in the presence of Tween 20 (black, blue and red curves). This peak is ascribed to the ester group in the surfactant Tween 20, providing evidence that Tween 20 adsorbs onto the AuNRs. This also suggests that the C-C component for the AuNRs PEGylated by our method (black curve) predominantly comes from the long alkyl chain of Tween 20 rather than CTAB, as no CTAB signal (N1s) is observed in Figure 2a. Compared with CTAB-capped AuNRs, the increase of C-O/C-C ratio following HS-PEG loading is indicative of the presence of $(-\text{CH}_2-\text{CH}_2-\text{O}-)_n$ repeating unit of PEG molecules⁴⁹ on the AuNRs.

As shown in Figure 2d, two Ag3d peaks (367.6 and 373.6 eV) are observed for all samples. The Ag content decreases significantly from CTAB-capped AuNRs (violet curve), to AuNRs prepared by the Liao method (green curve) and again to AuNRs PEGylated by our method (black curve). It has been reported that BSPP and NaCl can etch silver forming BSPP-Ag⁺ complex⁵⁰⁻⁵² and AgCl,^{51,53} respectively. The silver etching reaction with BSPP is competitive with the AuNR surface activation reaction illustrated in scheme 1b (step 2). The use of NaCl for silver etching promotes the AuNR surface activation, which explains the higher PEGylation efficiency in the presence of both BSPP and NaCl. Inductively coupled plasma mass spectrometry (ICP-MS) measurements show that ~25% of silver was removed from the AuNRs by our method. Further exposure of these AuNRs to an air-equilibrated water for two weeks, the Ag/Au ratio of the AuNRs (1.059%) remains almost unchanged, revealing that the most active silver atoms on the AuNR surface were removed during the PEGylation process. It is worth noting that the surface functionalization method developed here can also be extended to other surface ligands, such as thiol-PEG-carboxyl (Figure S6, Supporting Information). The direct exposure of positively charged CTAB-capped AuNRs to these negatively charged surface ligands involves a change of

surface charge from positive to negative. This results in the irreversible aggregation of AuNRs (Figure S6).

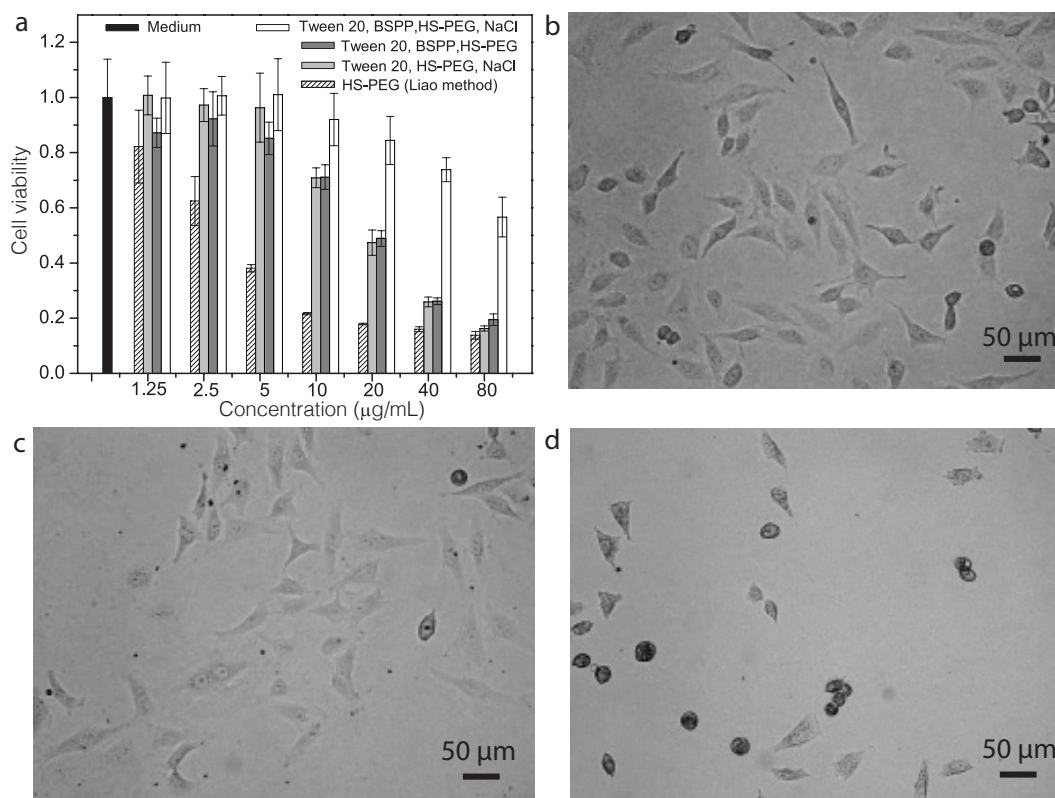


Figure 3. Cell viability: a) Dose-dependent cell viability of HeLa cells determined by the MTT assay after exposure to AuNRs for 24 h and optical images of HeLa cells treated with b) DMEM (control), c) 80 µg/mL of AuNRs PEGylated by our method and d) 80 µg/mL of AuNRs PEGylated by Liao method (incubation time: 4 hours). The AuNRs

As AuNRs have emerged as a new type of nanostructure for diagnostic and therapeutic applications,^{54,55} it is important to understand their potential risks to human health. Hence the *in vitro* cytotoxicity of the PEGylated AuNRs on HeLa cells (human cervical carcinoma cell line) using MTT-based colorimetric assay was examined. HeLa cells were chosen in our research as they are sensitive to CTAB.¹⁸ The cytotoxicity of the CTAB-capped AuNRs is not shown here

because these AuNRs completely precipitated in the cell culture medium (Dulbecco's modified Eagle's medium). Figure 3a shows the cell viability of HeLa cells as a function of AuNR concentration. The concentration of AuNRs was determined by UV-VIS spectroscopy based on the experimental extinction coefficient previously reported.¹² In this technique, the experimental extinction coefficient was calculated through the use of the real gold concentration determined by ICP measurements rather than the amount of gold precursor.¹² As presented in Figure 3a, the cell viability is critically dependent on the AuNR concentration and the amount of remaining CTAB and Ag on the AuNRs. The cell viability decreases with the increase in the amount of AuNRs. However, when using the same amount of AuNRs, the cell viability decreases with an increase in the amount of residual CTAB and Ag on the AuNRs. The AuNRs PEGylated by our method showed by far the lowest toxicity with no apparent toxicity when the AuNR concentration is below a concentration of 5 $\mu\text{g/mL}$. Even at a high AuNR concentration of 80 $\mu\text{g/mL}$, they still show a cell viability of $\sim 57\%$, which is four times higher than that ($\sim 14\%$) of the AuNRs PEGylated by the Liao method. The viability of HeLa cells was also recorded by the morphological criteria using optical microscope (Figure 3b-d). The majority of the cells treated with AuNRs PEGylated by our method (Figure 3c) show a typical spindle-like shape the same as those shown in the control experiment (Figure 3b), which is indicative of the cells being alive and healthy (AuNR concentration: 80 $\mu\text{g/mL}$, incubation time: 4 h). However, the cells incubated under the same conditions with AuNRs PEGylated by the Liao method (Figure 3d) are round in shape, which is a sign of cell death for HeLa cells. It is believed that the complete removal of CTAB and the most active silver on the surface layer of AuNRs are responsible for the high cell viability of the AuNRs PEGylated by our method.

4. CONCLUSIONS

In conclusion, we have developed a novel, simple, one-step surface modification method to produce biocompatible AuNRs. This was achieved by using a nonionic surfactant – Tween 20 to stabilize the AuNRs, BSPP to activate the AuNR surface for the subsequent PEGylation and NaCl to etch silver pre-deposited on the surface of AuNRs. This method allows for the complete functionalization of AuNRs with thiolated PEG and the removal of the most active silver on the AuNR surface. The PEGylated AuNRs show a significantly enhanced colloidal stability against a high concentration buffered saline solution and multiple rounds of centrifugation compared to CTAB-capped and partially modified AuNRs. We also investigated the cytotoxicity of the PEGylated AuNRs using HeLa cells as model cells. The AuNRs PEGylated by our method exhibit a complete detoxification at an AuNR concentration lower than 5 $\mu\text{g/mL}$. At a high concentration of 80 $\mu\text{g/mL}$, their cytotoxicity is about four times lower than that of the AuNRs PEGylated by the Liao method. Finally, this work represents a simple proof-of-concept experiment for the complete PEGylation and detoxification of CTAB-capped AuNRs. The surface modification method developed here can be easily extended to negatively charged surface ligands, e.g. thiol-PEG-carboxyl, and other NP systems with different compositions and shapes.

ASSOCIATED CONTENT

Supporting Information. AuNR PEGylation efficiency calculation, statistical analysis of AuNR's size and aspect ratio, optical and SEM images of AuNRs in coffee ring area, colloidal stability of AuNRs against centrifugation and high concentration buffered saline solutions, and surface elemental (XPS) and Raman spectroscopy analysis of PEGylated AuNRs. This material is available free of charge via the Internet at <http://pubs.acs.org>.

AUTHOR INFORMATION

Corresponding Authors

*Yuanhui.Zheng@unsw.edu.au

*Justin.Gooding@unsw.edu.au

ACKNOWLEDGMENT

The authors acknowledge the generous financial support from the Australian Research Council Industrial Transformation Training Centre for Advanced Technologies in Food Manufacture (IC130100021), Australian Research Council Centre of Excellence in Convergent Bio-Nano Science and Technology (CE140100036), UNSW Vice-Chancellor's Research Fellowship (RG134604), and the Australian Research Council through an Australian Research Fellowship (UB).

REFERENCES

- (1) Shi, C.; Soltani, S.; Armani, A. M. Gold Nanorod Plasmonic Upconversion Microlaser. *Nano Lett.* **2013**, *13*, 5827-5831.
- (2) Querejeta-Fernández, A.; Chauve, G.; Methot, M.; Bouchard, J.; Kumacheva, E. Chiral Plasmonic Films Formed by Gold Nanorods and Cellulose Nanocrystals. *J. Am. Chem. Soc.* **2014**, *136*, 4788-4793.
- (3) Tabor, C.; Van Haute, D.; A. El-Sayed, M. Effect of Orientation on Plasmonic Coupling between Gold Nanorods. *ACS Nano* **2009**, *3*, 3670-3678.
- (4) Zijlstra, P.; Paulo, P. M. R.; Orrit, M. Optical Detection of Single Non-absorbing Molecules Using the Surface Plasmon Resonance of a Gold Nanorod. *Nat. Nanotechnol.* **2012**, *7*, 379-382.
- (5) Yu, C.; Irudayaraj, J. Multiplex Biosensor Using Gold Nanorods. *Anal. Chem.* **2006**, *79*, 572-579.
- (6) Sönnichsen, C.; Alivisatos, A. P. Gold Nanorods as Novel Nonbleaching Plasmon-Based Orientation Sensors for Polarized Single-Particle Microscopy. *Nano Lett.* **2004**, *5*, 301-304.

- (7) Huang, H. C.; Rege, K.; Heys, J. J. Spatiotemporal Temperature Distribution and Cancer Cell Death in Response to Extracellular Hyperthermia Induced by Gold Nanorods. *ACS Nano* **2010**, *4*, 2892-2900.
- (8) Huang, X.; Neretina, S.; El-Sayed, M. A. Gold Nanorods: From Synthesis and Properties to Biological and Biomedical Applications. *Adv. Mater.* **2009**, *21*, 4880-4910.
- (9) Hauck, T. S.; Ghazani, A. A.; Chan, W. C. W. Assessing the Effect of Surface Chemistry on Gold Nanorod Uptake, Toxicity, and Gene Expression in Mammalian Cells. *Small* **2008**, *4*, 153-159.
- (10) Dickerson, E. B.; Dreaden, E. C.; Huang, X.; El-Sayed, I. H.; Chu, H.; Pushpanketh, S.; McDonald, J. F.; El-Sayed, M. A. Gold Nanorod Assisted Near-Infrared Plasmonic Photothermal Therapy (PPTT) of Squamous Cell Carcinoma in Mice. *Cancer Lett.* **2008**, *269*, 57-66.
- (11) Nikoobakht, B.; El-Sayed, M. A. Preparation and Growth Mechanism of Gold Nanorods (NRs) Using Seed-Mediated Growth Method. *Chem. Mater.* **2003**, *15*, 1957-1962.
- (12) Orendorff, C. J.; Murphy, C. J. Quantitation of Metal Content in the Silver-Assisted Growth of Gold Nanorods. *J. Phys. Chem. B* **2006**, *110*, 3990-3994.
- (13) Almora-Barrios, N.; Novell-Leruth, G.; Whiting, P.; Liz-Marzán, L. M.; López, N. Theoretical Description of the Role of Halides, Silver, and Surfactants on the Structure of Gold Nanorods. *Nano Lett.* **2014**, *14*, 871-875.
- (14) Liu, M.; Guyot-Sionnest, P. Mechanism of Silver(I)-Assisted Growth of Gold Nanorods and Bipyramids. *J. Phys. Chem. B* **2005**, *109*, 22192-22200.
- (15) Jackson, S. R.; McBride, J. R.; Rosenthal, S. J.; Wright, D. W. Where's the Silver? Imaging Trace Silver Coverage on the Surface of Gold Nanorods. *J. Am. Chem. Soc.* **2014**, *136*, 5261-5263.

- (16) Xiu, Z. M.; Zhang, Q. B.; Puppala, H. L.; Colvin, V. L.; Alvarez, P. J. J. Negligible Particle-Specific Antibacterial Activity of Silver Nanoparticles. *Nano Lett.* **2012**, *12*, 4271-4275.
- (17) Ma, R.; Levard, C.; Marinakos, S. M.; Cheng, Y.; Liu, J.; Michel, F. M.; Brown, G. E.; Lowry, G. V. Size-Controlled Dissolution of Organic-Coated Silver Nanoparticles. *Environ. Sci. Technol.* **2011**, *46*, 752-759.
- (18) Wang, L.; Liu, Y.; Li, W.; Jiang, X.; Ji, Y.; Wu, X.; Xu, L.; Qiu, Y.; Zhao, K.; Wei, T.; Li, Y.; Zhao, Y.; Chen, C. Selective Targeting of Gold Nanorods at the Mitochondria of Cancer Cells: Implications for Cancer Therapy. *Nano Lett.* **2010**, *11*, 772-780.
- (19) Alkilany, A. M.; Nagaria, P. K.; Hexel, C. R.; Shaw, T. J.; Murphy, C. J.; Wyatt, M. D. Cellular Uptake and Cytotoxicity of Gold Nanorods: Molecular Origin of Cytotoxicity and Surface Effects. *Small* **2009**, *5*, 701-708.
- (20) Niidome, T.; Yamagata, M.; Okamoto, Y.; Akiyama, Y.; Takahashi, H.; Kawano, T.; Katayama, Y.; Niidome, Y. PEG-Modified Gold Nanorods with a Stealth Character for *in vivo* Applications. *J. Controlled Release* **2006**, *114*, 343-347.
- (21) Bozich, J. S.; Lohse, S. E.; Torelli, M. D.; Murphy, C. J.; Hamers, R. J.; Klaper, R. D. Surface Chemistry, Charge and Ligand Type Impact the Toxicity of Gold Nanoparticles to *Daphnia Magna*. *Environmental Science: Nano* **2014**, *1*, 260-270.
- (22) Wang, L.; Jiang, X.; Ji, Y.; Bai, R.; Zhao, Y.; Wu, X.; Chen, C. Surface Chemistry of Gold Nanorods: Origin of Cell Membrane Damage and Cytotoxicity. *Nanoscale* **2013**, *5*, 8384-8391.
- (23) Cheng, X.; Zhang, W.; Ji, Y.; Meng, J.; Guo, H.; Liu, J.; Wu, X.; Xu, H. Revealing Silver Cytotoxicity Using Au Nanorods/Ag Shell Nanostructures: Disrupting Cell Membrane and Causing Apoptosis through Oxidative Damage. *RSC Advances* **2013**, *3*, 2296-2305.

- (24) Sanda, C. B.; Simion, A. Detoxification of Gold Nanorods by Conjugation with Thiolated Poly(ethylene glycol) and Their Assessment as SERS-Active Carriers of Raman Tags. *Nanotechnology* **2010**, *21*, 235601.
- (25) Kinnear, C.; Dietsch, H.; Clift, M. J. D.; Endes, C.; Rothen-Rutishauser, B.; Petri-Fink, A. Gold Nanorods: Controlling Their Surface Chemistry and Complete Detoxification by a Two-Step Place Exchange. *Angew. Chem. Int. Ed.* **2013**, *52*, 1934-1938.
- (26) Zhang, Z.; Lin, M. Fast Loading of PEG-SH on CTAB-protected Gold Nanorods. *RSC Advances* **2014**, *4*, 17760-17767.
- (27) Liao, H.; Hafner, J. H. Gold Nanorod Bioconjugates. *Chem. Mater.* **2005**, *17*, 4636-4641.
- (28) Dai, Q.; Coutts, J.; Zou, J.; Huo, Q. Surface Modification of Gold Nanorods through a Place Exchange Reaction Inside an Ionic Exchange Resin. *Chem. Commun.* **2008**, 2858-2860.
- (29) Thierry, B.; Ng, J.; Krieg, T.; Griesser, H. J. A Robust Procedure for the Functionalization of Gold Nanorods and Noble Metal Nanoparticles. *Chem. Commun.* **2009**, 1724-1726.
- (30) Sun, Z.; Ni, W.; Yang, Z.; Kou, X.; Li, L.; Wang, J. pH-Controlled Reversible Assembly and Disassembly of Gold Nanorods. *Small* **2008**, *4*, 1287-1292.
- (31) El Khoury, J. M.; Zhou, X.; Qu, L.; Dai, L.; Urbas, A.; Li, Q. Organo-Soluble Photoresponsive Azo Thiol Monolayer-Protected Gold Nanorods. *Chem. Commun.* **2009**, 2109-2111.
- (32) Khanal, B. P.; Zubarev, E. R. Angew. Rings of Nanorods. *Chem. Int. Ed.* **2007**, *46*, 2195-2198.
- (33) Vigderman, L.; Manna, P.; Zubarev, E. R. Quantitative Replacement of Cetyl Trimethylammonium Bromide by Cationic Thiol Ligands on the Surface of Gold Nanorods and Their Extremely Large Uptake by Cancer Cells. *Angew. Chem. Int. Ed.* **2012**, *51*, 636-641.

- (34) García, I.; Sánchez-Iglesias, A.; Henriksen-Lacey, M.; Grzelczak, M.; Penadés, S.; Liz-Marzán, L. M. Glycans as Biofunctional Ligands for Gold Nanorods: Stability and Targeting in Protein-Rich Media, *J. Am. Chem. Soc.* **2015**, *137*, 3686-3692.
- (35) Orendorff, C. J.; Alam, T. M.; Sasaki, D. Y.; Bunker, B. C.; Voigt, J. A. Phospholipid–Gold Nanorod Composites. *ACS Nano* **2009**, *3*, 971-983.
- (36) Takahashi, H.; Niidome, Y.; Niidome, T.; Kaneko, K.; Kawasaki, H.; Yamada, S. Modification of Gold Nanorods Using Phosphatidylcholine To Reduce Cytotoxicity. *Langmuir* **2005**, *22*, 2-5.
- (37) Yu, C.; Nakshatri, H.; Irudayaraj, J. Identity Profiling of Cell Surface Markers by Multiplex Gold Nanorod Probes. *Nano Lett.* **2007**, *7*, 2300-2306.
- (38) Harder, P.; Grunze, M.; Dahint, R.; Whitesides, G. M.; Laibinis, P. E. Molecular Conformation in Oligo(ethylene glycol)-Terminated Self-Assembled Monolayers on Gold and Silver Surfaces Determines Their Ability To Resist Protein Adsorption. *J. Phys. Chem. B* **1998**, *102*, 426-436.
- (39) Anstaett, P.; Zheng, Y.; Thai, T.; Funston, A. M.; Bach, U.; Gasser, G. Synthesis of Stable Peptide Nucleic Acid-Modified Gold Nanoparticles and Their Assembly onto Gold Surfaces. *Angew. Chem. Int. Ed.* **2013**, *52*, 4217-4220.
- (40) Cao, Y.; Jin, R.; Mirkin, C. A. DNA-modified Core-Shell Ag/Au Nanoparticles. *J. Am. Chem. Soc.* **2001**, *123*, 7961-7962.
- (41) Ford, M. J.; Masens, C.; Cortie, M. B. The Application of Gold Surfaces and Particles in Nanotechnology. *Surf. Rev. Lett.* **2006**, *13*, 297.
- (42) Gschneidner, T.; Moth-Poulsen, K. Handbook of Single Molecule Electronics, Pan Stanford Publishing Pte Ltd, **2009**; pp 23.

- (43) Hinterwirth, H.; Kappel, S.; Waitz, T.; Prohaska, T.; Lindner, W.; Lämmerhofer, M. Quantifying Thiol Ligand Density of Self-Assembled Monolayers on Gold Nanoparticles by Inductively Coupled PlasmaMass Spectrometry. *ACS Nano* **2013**, *7*, 1129-1136.
- (44) Nikoobakht, B.; El-Sayed, M. A. Evidence for Bilayer Assembly of Cationic Surfactants on the Surface of Gold Nanorods. *Langmuir* **2001**, *17*, 6368-6374.
- (45) Zheng, Y.; Rose L.; Thai, T.; Ng, S. H.; Eómez, D. E.; Ohshima, H.; Bach, U. Asymmetric Gold Nanodimer Arrays: Electrostatic Self-Assembly and SERS Activity. *J. Mater. Chem. A* **2015**,*3*, 240-249.
- (46) Zheng, Y.; Thai, T.; Reineck, P.; Qiu, L.; Guo, Y.; Bach, U. DNA-Directed Self-Assembly of Core-Satellite Plasmonic Nanostructures: A Highly Sensitive and Reproducible Near-IR SERS Sensor. *Adv. Funct. Mater.* **2013**, *23*, 1519-1526.
- (47) Thai, T.; Zheng, Y.; Ng, S. H.; Mudie, S.; Altissimo, M.; Bach. U. Self-Assembly of Vertically Aligned Gold Nanorod Arrays on Patterned Substrates. *Angew. Chem. Int. Ed.* **2012**, *51*, 8732-8735.
- (48) Ah, C. S.; Kim, W. J.; Yun, W. S.; Joo, S.W. Colorimetric Quantitative Sensing of Alkali Metal Ions Based on Reversible Assembly and Disassembly of Gold Nanoparticles. *Curr. Appl. Phys.* **2013**, *13*, 1889-1893.
- (49) Joshi, P. P.; Yoon, S. J.; Hardin, W. G.; Emelianov, S.; Sokolov, K. V. Conjugation of Antibodies to Gold Nanorods through Fc Portion: Synthesis and Molecular Specific Imaging. *Bioconjugate Chem.* **2013**, *24*, 878-888.
- (50) Lee, G. P.; Minett, A. I.; Innis, P. C.; Wallace, G. G. A New Twist: Controlled Shape-Shifting of Silver Nanoparticles from Prisms to Discs. *J. Mater. Chem.* **2009**, *19*, 8294-8298.

- (51) Xue, C.; Métraux, G. S.; Millstone, J. E.; Mirkin, C. A. Mechanistic Study of Photomediated Triangular Silver Nanoprism Growth. *J. Am. Chem. Soc.* **2008**, *130*, 8337- 8344.
- (52) Yang, J.; Lee, J. Y.; Too, H. P.; Valiyaveetil, S. A Bis(*p*-sulfonatophenyl)phenylphosphine-Based Synthesis of Hollow Pt Nanospheres. *J. Phys. Chem. B* **2006**, *110*, 125-129.
- (53) Ahern, A. M.; Garrell, R. L. In situ Photoreduced Silver Nitrate as a Substrate for Surface-Enhanced Raman Spectroscopy. *Anal. Chem.* **1987**, *59*, 2813-2816.
- (54) Murphy, C. J.; Sau, T. K.; Gole, A. M.; Orendorff, C. J.; Gao, J.; Gou, L.; Hunyadi, S. E.; Li, T. Anisotropic Metal Nanoparticles: Synthesis, Assembly, and Optical Applications. *J. Phys. Chem. B* **2005**, *109*, 13857-13870.
- (55) Jain, P. K.; Lee, K. S.; El-Sayed, I. H.; El-Sayed, M. A. Calculated Absorption and Scattering Properties of Gold Nanoparticles of Different Size, Shape, and Composition: Applications in Biological Imaging and Biomedicine. *J. Phys. Chem. B* **2006**, *110*, 7238- 7248.

TOC Graphic

